

Regular Paper

Particle Tracking Velocimetry Applied for Fireworks

A Demonstration of Vector Field Measurement in Hundreds Meter Space

Murai, Y.* , Oishi, Y.* , Tasaka, Y.* and Takeda, Y.*

* Division of Energy and Environmental Systems, Graduate School of Engineering, Hokkaido University, Sapporo, 060-8628, Japan. E-mail: murai@eng.hokudai.ac.jp

Received 18 July 2007
Revised 30 October 2007

Abstract: Particle tracking velocimetry (PTV) is applied for measuring the motions of luminous particles in fireworks. The objective of the study is to clarify the technical problems encountering in large-scale quantitative visualization in natural environment. The major problems are found to be uncontrolled background in nature, low pixel resolution relative to particle size, and large perspective. The ways to deal with these problems in current technological level are discussed. In the application, two cameras are located at 1.3 km from the launching point with 30-degree opening angle to implement 3-D PTV. The transient 3-D velocity distributions of around 200 m-scale diameter fireworks are obtained during the light emission from the explosion till burnout. Moreover, the evolution of the mean particle diameter that decreases continuously with the combustion is estimated with the measured velocity information by the particle's equation of motion.

Keywords: Visualization, PTV, Telescopic Imaging, Firework, And Three-Dimensional Flow.

1. Introduction

Measurement methods for large-scale flow is demanded in order to assess the environmental issue of our activity. These arise in particular for predicting and analyzing transient wind flow that governs diffusion of poisonous substances, wind turbine performance, and local damage estimation due to storms or tornados. The length scale of interest here ranges from 100 m to 1 km, which is unresolved directly in satellite images. Modern technologies dealing with this flow scale are known to use electromagnetic wave emitted to atmosphere, such as by Doppler radar velocimetry (Elliot and Beutner, 1999). The aim of the present study is to find technical problems when particle tracking velocimetry (PTV) based on ordinary visible light is applied for acquiring 3-D vector field of hundreds meter scale.

PTV is nowadays well-established technology as one of particle image velocimetries (PIV) (Adrian, 2005). The strongest advantage of PTV is of fine spatio-temporal resolution since it directly tracks individual particle motions. Use of plural cameras enables us to extend it to three-dimensional three-component (3-D 3-C) velocity measurement (Nishino et al., 1989). With these advantages of PTV one advances to micro-fluid dynamics that includes topics in bio/chemistry for finding out non-Newtonian fluid properties and micro-thermofluid characteristics (Santiago et al., 1998). In this field, lens optics is a major interest both for their utilization and error estimation. Another advance is to extend PTV toward large flow field measurement in natural environment. There are papers in the past on the flow having a tens of meter range (Weitbrecht et al., 2002). For large scale flow over 100 m, the problems would be 1) seeding in wide space, 2) outdoor illumination, 3) imaging with large perspective magnification, and 4) tracking of high-speed particles.

In the present study, fireworks - “Hanabi” in Japanese- are chosen as a target to be discussed by focusing on the items 3) and 4) among above. It is of course noted that the light-emitting particles of fireworks have large inertia given by the initial explosion so that they are considered to be inadequate as an airflow tracer. Instead, the time evolutions of the particle size and the combustion rate during the flowering can be estimated with particle’s equation of motion using the PTV data. We report these problems and solutions in this paper.

2. Measurement Method

2.1 Acquisition of Firework Image

Fireworks are recorded by two cameras located at distances more than 1 km from the launching point. The target is firework festival held in Sapporo City, Japan, during evening time from 19 to 21 O’clock in summer. The left picture of Fig. 1 shows the details of geometrical conditions. The viewing angles of two cameras relative to horizontal plane are 0.0 degree for the camera A (set on the roof of a high-building apartment house), and 5.0 degree for the camera B (set on a high elevation hill in a park), respectively. The field of view is set as 300 m in the vertical direction in order to capture 200 m-scale fireworks. The cameras (Sony, DCR-VX2100, 3-CCD, 640 x 480 pixel) record them at 30 fps in frame rate and 1/250 s in shutter speed, and operated independently because of too long distance to be connected for synchronization. The lenses used are 58 mm in diameter, and 1.6 in F -number. The perspective magnification factor ranges from 0.54 to 0.66 m/pixel. The synchronized pair of the stereoscopic images are obtained in the stage of image analysis using the time-code provided in the digital video files, and also verified by the frame timing of the initial light-emission of the firework. In summary, the space and time resolutions are 0.21 m³/voxel and 1/60 s (half the sampling time interval), respectively.

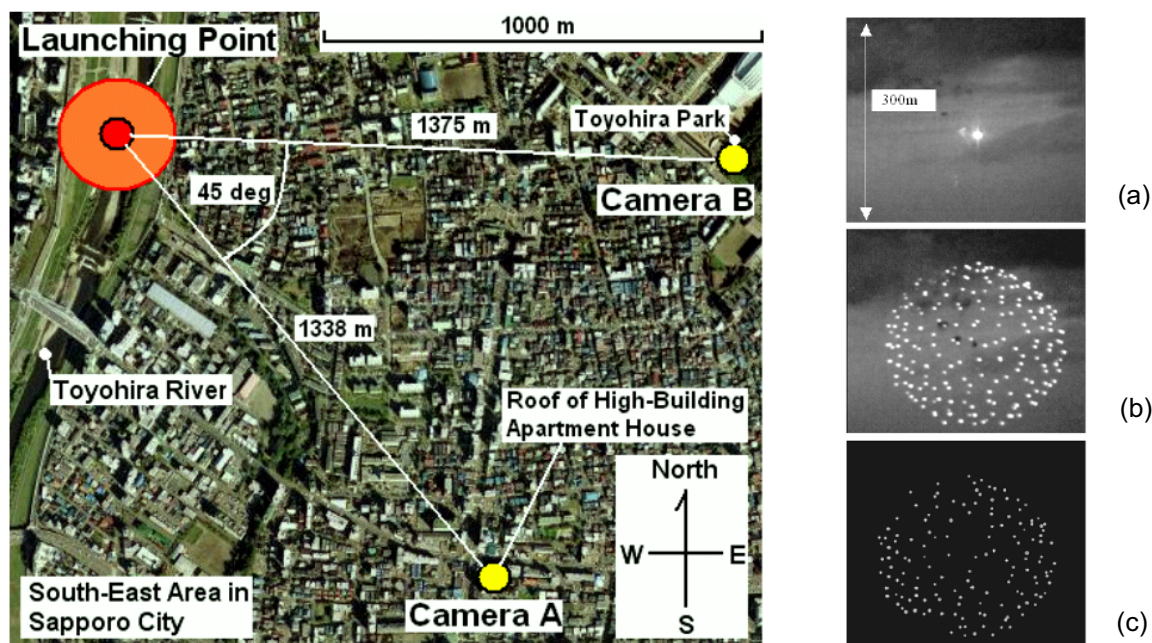


Fig. 1. Photographing conditions and images of fireworks: (a) The moment of explosion, (b) the moment of brightest flowering, (c) the particles detected.

2.2 Particle Tracking Velocimetry

Four-step tracking algorithm is applied to capture the velocity vectors of individual particles. This algorithm works well for the present type of particle motions that are dominated by the inertia and is less affected by the fluctuation of ambient fluid flow. Namely the particles have higher intrinsic property in time direction than in spatial correlation. Particle displacement per frame is within 50 pixels except a few initial frames just after the explosion. Only a few erroneous vectors are resulted by miss-tracking out of hundreds particles.

In the application of PTV for fireworks, the following points should have been dealt with. The first problem that we experienced is how the individual particles are detected from the image. This problem consists of two factors; 1) subtraction of the natural background, and 2) the particle size relative to pixel resolution. For the 1st matter, ordinary background subtraction, i.e., taking differential image from non-particle image, can be applied to the firework image when the natural background moves little. However, the particles emit light in moving natural background such as in bright cloud as shown in Figs. 1(a) and (b). During our recording of the firework, the wind speed was approximately 5 m/s as the estimate from the cloud advection. This corresponds to 170 mm displacement per frame, being much larger than the particle size. Hence our approach employs the dynamic minimum brightness distribution as the substantial background image for the particle detection, i.e., the temporal minimum brightness distribution during the time within $t-\tau/2 < t < t+\tau/2$. Here, τ is the control period which is chosen enough short so that the cloud is treated as temporally frozen background. It is undoubtedly noted that the particles after their end of combustion cannot be detected by any of background subtraction. The second matter, i.e., the pixel resolution is a more serious experience we encountered. The magnification factor ranges from 0.54 to 0.66 m/pixel, and thus the particle size of around 30 mm is unresolved. This point can be ignored if recorded fireworks are simply replayed on the display for enjoying purpose. For particle tracking velocimetry, however, this insufficient resolution results in a lack of time-continuous trajectories and drastic decrease in the number of vectors to be acquired. The optical condition in exact focusing even worsens the performance and gets more insensitive to the CCD-aperture array. In order to overcome this fatal problem, we have applied defocus condition to cast all the particles on the image (see Fig. 1(b)). The defocusing makes the particle size on the image plane expand up to 5 pixels so that flicker of moving particles ceases. The particles are detected from the original gray level images by binarization with an adequate brightness threshold. The centers of the individual particle are calculated for all the image objects remained after the binarization. A sample of detected particles is shown in Fig. 1(c).

2.3 Stereoscopic Data Analysis

Optical geometry calibration is implemented after two-dimensional velocity vector data are obtained from the images of cameras A and B, respectively. The calibration is for a perspective correction based on pinhole camera model as shown in Fig. 2. The model considers the following factors: rotation angles about viewing axes relative on co-planer meridian coordinate of the two cameras $\{\omega, \phi, \chi\}$ cross-angle between the viewing axes $\{\theta\}$ and individual magnification factors $\{m_L, m_R\}$. The particle coordinates on physical space $\{X, Y, Z\}$ are obtained from their image coordinates $\{x_L, y_L, x_R, y_R\}$ via the relative coordinate $\{x'_L, y'_L, x'_R, y'_R\}$ as below.

$$\begin{pmatrix} x'_L \\ y'_L \\ z'_L \end{pmatrix} = \begin{pmatrix} x_L \\ y_L \\ -C_L/m_L \end{pmatrix} \quad (1)$$

$$\begin{pmatrix} x'_R \\ y'_R \\ z'_R \end{pmatrix} = \begin{pmatrix} 1 & 0 & 0 \\ 0 & \cos \omega & -\sin \omega \\ 0 & \sin \omega & \cos \omega \end{pmatrix} \begin{pmatrix} \cos \phi & 0 & \sin \phi \\ 0 & 1 & 0 \\ -\sin \phi & 0 & \cos \phi \end{pmatrix} \begin{pmatrix} \cos \chi & -\sin \chi & 0 \\ \sin \chi & \cos \chi & 0 \\ 0 & 0 & 1 \end{pmatrix} \begin{pmatrix} x_R \\ y_R \\ C_R/m_R \end{pmatrix} + \begin{pmatrix} 0 \\ b_y \\ b_z \end{pmatrix} \quad (2)$$

$$\begin{pmatrix} X \\ Y \\ Z \end{pmatrix} = \begin{pmatrix} m_L & 0 & 0 & 0 \\ -m_L/\tan \theta & 0 & m_R/\cos(\pi/2-\theta) & 0 \\ 0 & m_R/2 & 0 & m_R/2 \end{pmatrix} \begin{pmatrix} x'_L \\ y'_L \\ x'_R \\ y'_R \end{pmatrix} \quad (3)$$

$$\begin{pmatrix} U \\ V \\ W \end{pmatrix} = \frac{1}{\Delta t} \begin{pmatrix} m_L & 0 & m_R \cos \theta & 0 \\ m_L \sin \theta & 0 & 0 & 0 \\ 0 & m_L/2 & 0 & m_R/2 \end{pmatrix} \begin{pmatrix} \Delta x'_L \\ \Delta y'_L \\ \Delta x'_R \\ \Delta y'_R \end{pmatrix} \quad (4)$$

Here C_L and C_R are the distance from each camera to the cross point of two viewing axes, respectively. The values b_y and b_z are correction distances for the angle difference, $\beta - \alpha$. The symbol Δ denotes the interval values between two image frames. When the stereo-matching is applied with Eq. (3) to get the three-dimensional particle coordinates, the poor pixel resolution relative to the particle size becomes a new problem that should be overcome. Generally we need to allow the pair-matching process to have a tolerance for the uncertainty in the optical geometry. The tolerance must be reduced in accordance with the number of particles in the image. However, poor pixel resolution in each image leads to a large voxel uncertainty to be competitive to the tolerance. The accuracy in particle position is known as half the voxel, i.e., 0.3^3 m^3 in the present case, and the algebraic pair-matching is unavailable below this criterion. Many possible particles fulfill the pair condition due to large voxel, resulting in a plenty number of so-called ghost particles in the reconstructed three-dimensional space. Therefore, much higher resolution is required in order to reduce the ghost particles, such as by use of high-definition camera with progressive scanning function.

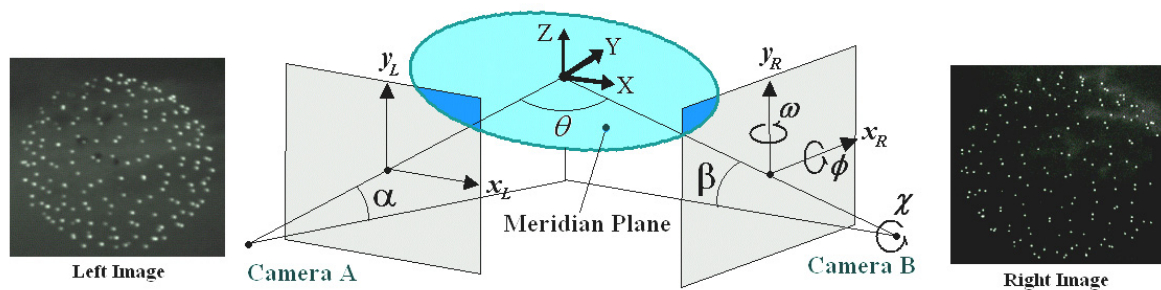


Fig. 2. Stereo-matching of two PTV data to obtain three-dimensional velocity vectors of firework particles.

3. Results and Discussions

3.1 Velocity Vector Field of Particles

Figure 3 shows the velocity vector distributions obtained by 3-D PTV. The time T is the time from the explosion until the complete disappearance of light emission at 1.70 s. As shown in the light column, the particle velocity at $T = 0.34$ s is larger than 50 m/s. The velocity decreases while the particles scatter in the radial direction. The velocity vectors start to be oriented downward due to gravity near in the end of light emission at $T = 1.36$ s.

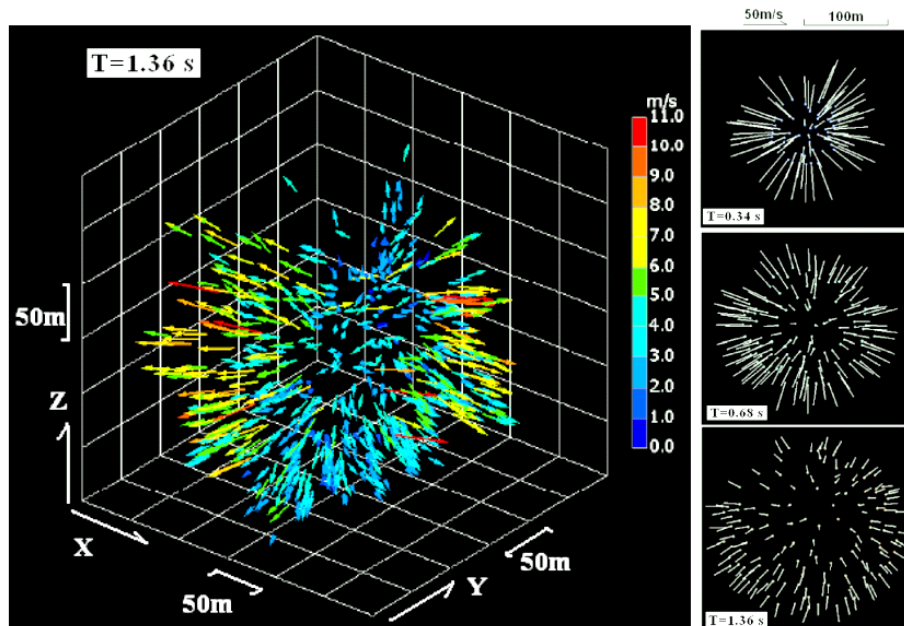


Fig. 3. Instantaneous velocity vector distributions acquired by 3-D PTV.

Figure 4(a) shows trajectories of individual particles during the lifetime of the firework. The coloring from blue to red is defined as the time from the explosion, being different from the true color of light. As shown by this, the flying particles slowly descend with gravity when the inertia given by the initial explosion is consumed by the drag.

Figure 4(b) shows the performance of stereo-pair matching, which are evaluated by the number of particles in four categories. The number of detected particles in Camera A is larger than in Camera B. This is owing to differences in the particle contrast relative to each background image and also in defocusing condition. Such a difference is a typical result in wide-space PTV measurement in natural environment, but cannot be excluded completely. The number of 3-D matched particles is larger than the number of particles detected in Camera B because of the given voxel tolerance. This indicates simultaneously that there are many ghost particles that fulfill the matching condition but do not exist in true physical space. As mentioned in section 2.3, a pair of cameras with higher resolution is required to reduce the ghost particles. In our data analysis, the ghost particles are removed by judging the direction of velocity vector that should at least orient outward from the center.

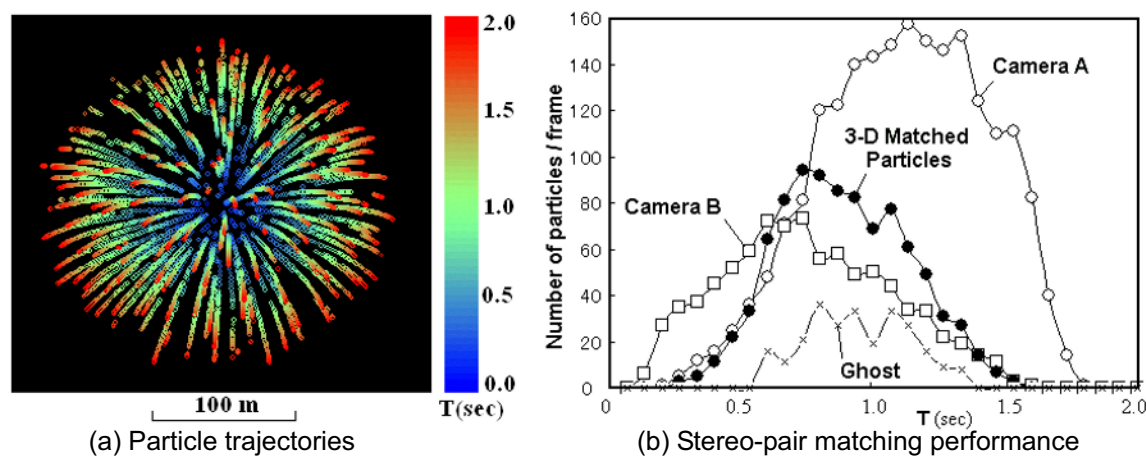


Fig. 4. Detection of three-dimensional velocity vectors.

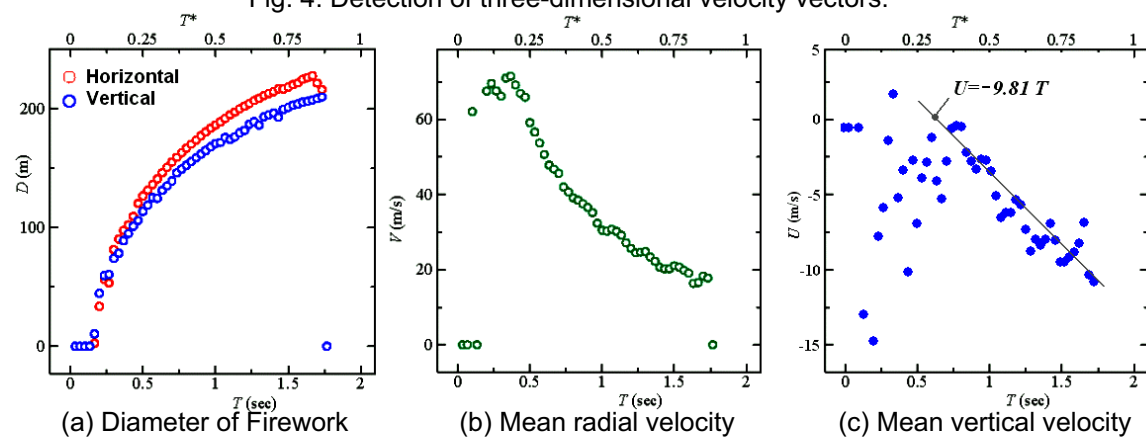


Fig. 5. Representative factors of firework measured by velocity vector field.

Figure 5(a) shows the time evolution of the firework diameter, which is estimated by the particle coordinates. The diameter is classified into the horizontal and the vertical ones since the outline is non-spherical. The both diameters increase rapidly after the explosion at $T = 0$ s and become eventually larger than 200 m at around $T = 1.5$ s. The vertical diameter is 10 %-smaller than the horizontal one. This is explained by the drag acting on the fast-moving particles in the air, i.e., the particle receives the drag in proportional to the velocity squared that is asymmetric in the vertical direction when the particles have initial vertical velocity on the moment of explosion or the particles are accelerated by gravity during their scattering. The isolated plot at $(T, D) = (1.75 \text{ s}, 0 \text{ m})$ means the final light emitting particle remained in the image. Figure 5(b) shows the time evolution of the particle's mean radial velocity sampled from the PTV data. The velocity decreases nearly

inversely proportional to time for $T > 0.5$ s due to drag against the air. The instantaneous maximum velocity is obtained as 70 m/s at $T = 0.4$ s. However, the real maximum velocity is known to be around 100 m/s according to the momentum theory of particles that are accelerated by high pressure gradient during the explosion (Hosoya, 1999). The theory further explains that the effective acceleration time by the explosion pressure is within 0.05 s. Extrapolating the present velocity evolution to backward in time estimates the maximum velocity as 100 m/s at $T = 0.05$ s. The reason of the failed detection for $T < 0.05$ s is too low light emission because of null combustion in the beginning of the firework. This is also why the diameter was measured to be 0 m for $T < 0.2$ s in Fig. 5(a). Figure 5(c) shows the mean vertical velocity which generally follows acceleration of gravity at $T > 0.75$ s, i.e., $U = -9.81$ T. The large deviation of the velocity in the initial half of the flowering at $T < 0.75$ s causes owing to the velocity difference provided randomly by the initial explosion.

The above quantities are the most representative characterization of the firework dynamics. Other evaluation is also possible when the PTV data are analyzed for a given purpose. In this paper, as one of the most interesting demonstrations in utilization of the measured velocity, we focus on the combustion behavior that can be also extracted from the velocity vector information as below.

3.2 Analysis of Particle Motion

Equation of motion for a single solid spherical particle in quiescent fluid is expressed by

$$m_p(t) \frac{d\mathbf{u}_p}{dt} = -C_D \pi r_p(t)^2 \frac{1}{2} \rho_f |\mathbf{u}_p| \mathbf{u}_p - \frac{4}{3} \pi r_p(t)^3 \nabla p - m_p(t) \mathbf{g} \quad (5)$$

here m_p , u_p and r_p , are mass, velocity, and radius of the particle. C_D , ρ_f , p and g are drag coefficient, density of surrounding fluid, pressure, and acceleration of gravity. Namely this equation considers inertia, drag, pressure gradient, and gravity acting on the particle. In the firework, the velocity component u_p on the horizontal plane that crosses the center of firework is given by

$$\frac{du_p}{dt} = -\frac{1}{m_p(t)} C_D \pi r_p(t)^2 \frac{1}{2} \rho_f u_p^2 \rightarrow \frac{du_p}{dt} = -\alpha(t) u_p^2, \quad \alpha(t) = \frac{8C_D}{3r_p(t)} \frac{\rho_f}{\rho_p} \quad (6)$$

This equation is derived so since gravity does not act in the horizontal direction. In addition, we assume that the local pressure gradient in the sky is dispensable for inertia dominant behavior of high-speed flying particles. The parameter α is a function of the particle radius that changes with time due to combustion. When the particle's horizontal velocity u_p is measured, α is calculated only from the velocity and thus the particle radius is estimated by,

$$r_p(t) = \frac{1}{\alpha(t)} \left(\frac{8\rho_f}{3\rho_p} C_D \right), \quad \alpha(t) = -\frac{1}{u_p^2} \frac{du_p}{dt} \quad (7)$$

Here the drag coefficient in Reynolds region is constant and is given by $C_D = 0.5$ for $10^4 < \text{Re} < 2 \times 10^5$. The density ratio is $\rho_p/\rho_f = 1196$ (Hosoya, 1999). Because of certain measurement error in u_p , the parameter α is inaccurate if the original measurement value is directly used in Eq. (7). Therefore the following approximation function is assumed as the velocity evolution in order to reduce the influence of the error.

$$u_p(t) = u_{p1} \left\{ \left(\frac{t-t_1}{t_2-t_1} \right)^n \left(\frac{u_{p1}}{u_{p2}} - 1 \right) + 1 \right\}^{-1}, \quad t_1 \leq t \leq t_2 \quad (8)$$

here the suffixes 0 and 1 stand for two instants during the particle dispersion. The index n is calculated by least square method and obtained to be $n = 1.25$ for $0.5\text{s} < t < 1.7\text{s}$. After the particle radius $r_p(t)$ is obtained, the combustion rate is calculated by

$$\dot{m} = -\frac{dm_p}{dt} = -\frac{d}{dt} \left(\rho_p \frac{4}{3} \pi r_p^3 \right) = -4\pi r_p^2 \rho_p \frac{dr_p}{dt} \quad (9)$$

which is defined by the particle's mass reduction per unit time.

Figure 6 shows the particle diameter and the combustion rate estimated by Eqs. (7), (8) and (9). The particle diameter is estimated to be 10 to 25 mm in the period analyzed. In the firework ball, the particles are packed in a single layer as shown in Fig. 6(b), and its original diameter is 30 mm. Hence the estimated range of the diameter agrees well with it. However, the decrease of the diameter become weak for $t > 1.0$ s and remains to be 10 mm at the moment of light emission out at $t = 1.7$ s. This diameter at light-off moment is somewhat difficult to be believed immediately, however, it is consistent to the measured combustion rate that drops sharply during the flowering and becomes nearly zero soon. This result indicates that the combustion rate is highly dominated by the particle velocity that is also quickly reduced by the drag against the air. After $t = 1.7$ s, we suppose that a little combustion continues further to reduce the diameter. The light emission with very low brightness is insensitive to the CCD camera, and is hence not recorded in the images. The disappearance of the particles in the flowering-end is also explained by the long perspective photographing. Reminding that the magnification factor is around 0.6 m/pixel, it is understood that the firework particles smaller than 10 mm are buried in the background image. Nevertheless, we have to emphasize that these quantities are all estimated only by the velocity information that is measured by the wide perspective stereoscopic imaging system. Without PTV-based information, it is obviously impossible to directly measure the diameter and the combustion rate of 200 m-scaled fireworks on given pixel and gray level resolutions. In this sense the large-scale PTV provides beneficial information via the velocity data and can be a general tool for indirect measurement of flying objects.

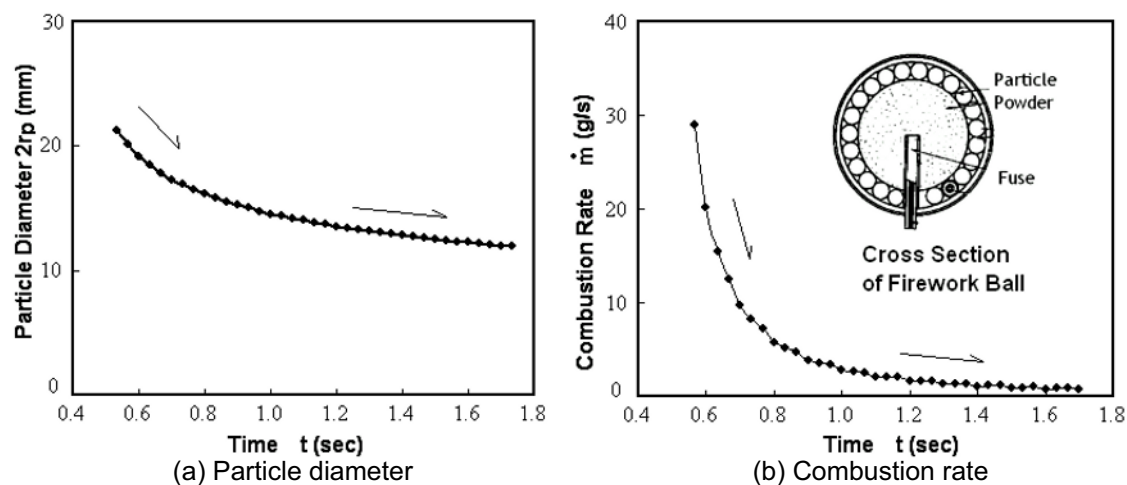


Fig. 6. Particle diameter and combustion rate estimated by PTV measurement data.

4. Conclusion

Technical problems of particle tracking velocimetry in the application to hundreds meter scale in natural environment are reported in this paper. Through the demonstration by stereoscopic firework measurement, the most serious problem is a low voxel resolution relative to the particle size, which generates many flickering/ghost particles in 3-D matched space. Nevertheless, the quantitative characterization was successful to understand the behavior of 50 m/s-order high-speed particles, which is represented by the outline firework diameter, the particle velocity, the particle diameter and the combustion rate. The experience and knowledge obtained in this study will be utilized to the next stage of the application that we plan to do for atmospheric turbulence and tornado dynamics.

Acknowledgment

The authors thank to Dr. M. Mori and Mr. H. Tezuka for the grant supported by Tokyo Electric Power Cooperation. They also appreciate to Mr. M. Morinaga, a former graduate course student of Hokkaido University, for his helps with image acquisition and analysis.

References

- Adrian, R. J., Twenty Years of Particle Image Velocimetry, *Experiments in Fluids*, 39 (2005), 159-169.
- Elliot, G. S. and Beutner, T. J., Molecular Filter Based Planer Doppler Velocimetry, *Progress in Aerospace Sciences*, 35 (1999), 799-845.
- Hosoya, M. and Hosoya F., *Science in Fireworks*, (1999), 44-48, 115-115, 159-166, Tokai Library Press (in Japanese).
- Nishino, K., Kasagi, K. and Hirata, M., Three-dimensional Particle Tracking Velocimetry Based on Automated Digital Image Processing, *ASME J. Fluids Engineering*, 111 (1989), 384-391.
- Santiago, J. C., Meinhart, C. D., Wereley, S. T., Beebe, D. J. and Adrian, R. J., A Particle Image Velocimetry System for Microfluidics, *Experiments in Fluids*, 25 (1998), 316-319.
- Weitbrecht, V., Kuehn, G. and Jirka, G. H., Large Scale PIV Measurement at the Surface of Shallow Water Flows, *Flow Measurement and Instrumentation*, 13 (2002), 237-245.

Author Profile



Yuichi Murai: He received his M.Sc. (Eng) in Mechanical Engineering in 1993 from University of Tokyo. He also received his Ph.D. in Mechanical Engineering in 1996 from University of Tokyo. He worked in Department of Mechanical Engineering, Fukui University as a research associate from 1995 to 2000. He worked in Imperial College, University of London for 2001-2002 as a JSPS fellow, and works in Graduate School of Engineering, Hokkaido University since 2003 as an associate professor. His research interests are PIV, multiphase flow, turbulent flow, bubble dynamics, drag reduction, and new fluid machinery.



Yoshihiko Oishi: He received his M.Sc. (Eng) in Fiber Amenity Engineering in 2005 from Fukui University. He is now studying as a Ph.D course student in Division of Energy and Environmental Systems, Graduate School of Engineering, Hokkaido University, Japan, and researching application of PIV to multiphase flows as a JSPS(Japan Society for the Promotion of Science) research fellow. His research interests are drag reduction, PIV, multi-phase flow, turbulent flow, and bubble dynamics.



Yuji Tasaka: He received his M. Eng. in Mechanical Engineering in 2002 from Hokkaido University. He also received his Ph.D. in Mechanical Engineering in 2005 from the same university. He worked in the Graduate School of Engineering, Hokkaido University as a research associate. He is an assistant professor since 2006. His research interests are ultrasonic measurement of liquid metal flow, especially thermal convection, flow instability and transition processes from laminar flow to turbulent flow.



Yasushi Takeda: He received his M.Sc. (Eng) in Engineering School in 1970 from Tohoku University, and received his Ph.D. (Eng) in 1979 from the same university. He worked in Department of Engineering, Tohoku University as an instructor till 1981 and then moved to Swiss Institute for Nuclear Research. He worked in Paul Scherrer Institute Switzerland as a Senior Researcher since 1988 before he became a professor of Hokkaido University. During his long visit in PSI he received his second title of Ph.D(Science) from The University of Tokyo in 1996. His research interests are ultrasonic velocity profiling(UVP), flow measurement methodology, vortex dynamics and transition to turbulence.